

Multi-wavelength observations of stellar populations in Galactic globular clusters

F. R. Ferraro

*INAF-Osservatorio Astronomico di Bologna, via Ranzani 1, 40127
Bologna, Italy*

Abstract. I report on some recent results in the framework of a complex project aimed to characterize the photometric properties of stellar populations in Galactic Globular Clusters.

1. Introduction

Galactic globular clusters (GGCs) are extremely important astrophysical objects since *(i)* they are prime laboratories for testing stellar evolution; *(ii)* they are “fossils” from the epoch of galaxy formation, and thus important cosmological tools; *(iii)* they serve as test particles for studying the dynamics of the Galaxy. A few years ago our group started a long-term project devoted to study the global stellar population in a sample of “proto-type” GGCs following a multi-wavelength approach: IR and optical observations to study cool giants and UV observations to study blue hot sequences (Horizontal Branch (HB), Blue Stragglers Stars (BSS), etc). In this paper I report a short summary of the most recent results.

2. Calibrating the photometric properties of the Red Giant Branch in the IR

The advantage of observing cool giants in the near IR is well known since many years. The contrast between the red giants and the unresolved background population in the IR bands is greater than in any optical region, so they can be observed with the highest S/N ratio also in the innermost region of the cluster. Moreover, when combined with optical observations, IR magnitudes provide useful observables such as the V–K color, an excellent indicator of the stellar effective temperature (T_e), and allows a direct comparison with theoretical model predictions. Since the peonering work by Frogel and collaborators (Frogel, Cohen & Persson 1983) in the early 80’s, many groups have performed systematic IR observations in (mainly) heavily-obscured GGCs (see Frogel et al. 1995; Kuchinski & Frogel, 1995; Minniti et al. 1995; Davidge 2000; Ortolani et al. 2001).

In Ferraro et al. (2000, hereafter F00) a new set of high quality near-IR Color Magnitude Diagrams (CMDs) was presented for a sample of 10 GGCs, spanning a wide range in metallicity. We used this homogeneous data-base to define a variety of observables allowing the complete characterization of the pho-

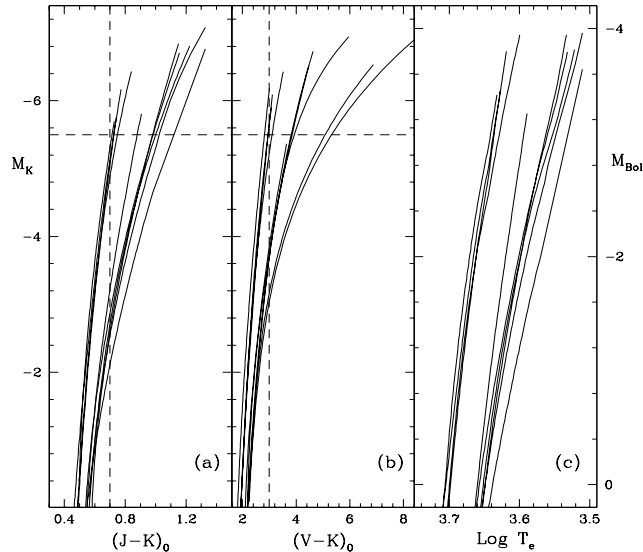


Figure 1. RGB fiducial ridge lines for the 10 GGCs in the F00 sample in the $M_K, (J-K)_0$, $M_K, (V-K)_0$ and $(M_{Bol}, \text{Log}(T_e))$ planes, (*panel (a)*, (*b*) and (*c*)), respectively. The dashed lines indicate the magnitude levels at which some of the parameters defined in F00 are measured.

tometric properties of the Red Giant Branch (RGB), namely: (*a*) the location of the RGB in the CMD both in $(J-K)_0$ and $(V-K)_0$ colors at different absolute K magnitudes (-3 , -4 , -5 , -5.5) and in temperature; (*b*) its overall morphology and slope; (*c*) the luminosity of the Bump and of the Tip. All these quantities have been measured with a homogeneous procedures applied to each individual CMD by adopting the distance moduli scale defined in Ferraro et al. (1999a, hereafter F99). The mean ridge lines for the selected clusters, in various planes are shown in Figure 1.

A set of relations linking the photometric parameters to the cluster global metallicity ($[M/H]$, see F99) has been obtained in F00. Such a set of equations can be very useful to derive photometric estimates of the metallicity distributions in complex, *i.e.* chemically inhomogeneous, stellar populations as those observed in nearby dwarf galaxies. Indeed, one of the most puzzling (and nearest) examples of complex stellar population is just in the Halo of the Galaxy: the cluster ω Centauri.

ω Centauri is the most massive globular cluster of the Milky Way ($3 \times 10^6 M_\odot$), and it is the only known galactic globular which shows clear and undisputed variations in the heavy elements content of its giants. Recent wide field photometric surveys (Lee et al. 1999, Pancino et al. 2000) have shown the existence of a previously unknown anomalous RGB (RGB-a). We have recently obtained extensive J,K observations in a wide region ($13' \times 13'$) around the cluster center. Figure 2 (*left panel*) shows the CMD obtained combining IR observations with the optical catalog by Pancino et al (2000). The mean ridge line of the dominant (metal poor) population and of the anomalous RGB-a (metal rich) population are overplotted to the CMD, and compared (in Figure 2-*left panel*)

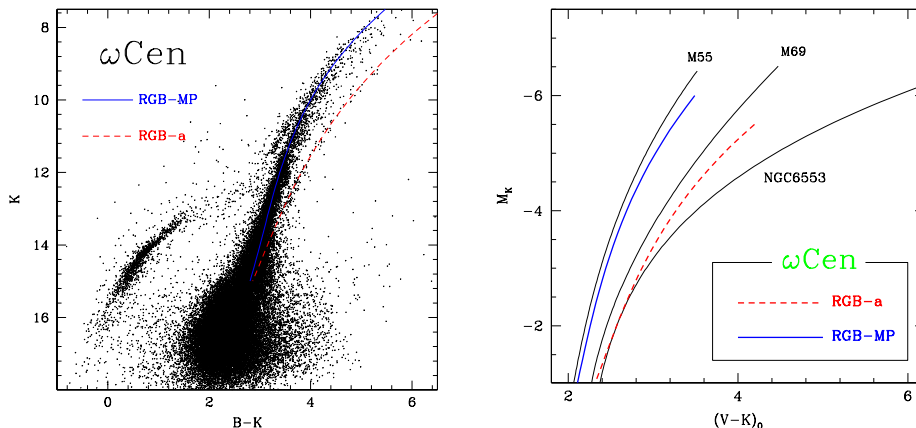


Figure 2. *Left panel:* $(K, B - K)$ -CMD for more than 50,000 stars in the central region of ω Cen. The RGB mean ridge line of the metal poor and the anomalous population are overplotted. *Right panel:* The mean ridge lines of the metal poor (solid line) and the anomalous population (dashed line) are compared with the RGB ridge lines of M55, M69 and NGC6553 from F00.

with the mean ridge lines of three reference clusters (from F00). The shape of the RGB-a and its position in the CMD indicate a metallicity of $[M/H] \sim -0.5$, which is fully consistent with the most recent direct spectroscopic determination (Pancino et al 2002).

3. Mid-IR Observations of GGCs: probing the mass loss process along the Red Giant Branch

A complete, quantitative understanding of the physics of mass loss processes and the precise knowledge of the gas and dust content in GGCs is crucial in the study of Population II stellar systems and their impact on the Galaxy evolution. Despite its importance, mass loss is still a poorly understood process.

In order to shed some light on mass loss processes along the RGB we performed (Origlia et al 2002) a deep Mid-IR survey with ISOCAM of the very central regions of six, massive clusters: 47 Tuc, NGC 362, ω Cen, NGC 6388, M15 and M54. Mid-IR observations are the ideal tool to study mass loss, since they could detect an outflowing gas fairly far away from the star (typically, tens/few hundreds stellar radii).

Two different filters ($[12]$, $[9.6]$) in the $10 \mu\text{m}$ spectral region have been used. The mid-IR colors have been then combined with near-IR colors in order to obtain photometric indices ($K - [12]$ or $K - [9.6]$), which are sensible tracers of circumstellar dust excess. Figure 3 shows the M_{bol} , $(J - K)_0$ and M_{bol} , $(K - [12])_0$ CMDs. Stars with $(K - [12])_0 \geq 0.65$ are classified as sources with significant dust excess and are marked with filled symbols in the Figure.

There are a series of interesting results suggested by this Figure: (i) all the stars showing evidence of mid-IR circumstellar dust excess are in the upper 1.5

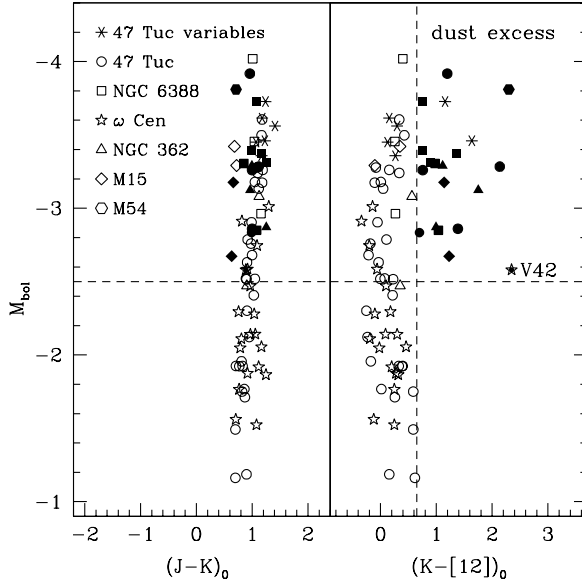


Figure 3. M_{bol} , $(J - K)_0$ (left panel) and M_{bol} , $(K - [12])_0$ (right panel) de-reddened CMD of the ISOCAM point sources detected in six globular clusters (from Origlia et al 2002). Sources with $(K - [12])_0 \geq 0.65$ (dashed vertical line) are classified as sources with significant dust excess and are marked with filled symbols.

bolometric magnitudes of the RGB, suggesting that *significant mass loss occurs only at the very end of the RGB evolutionary stage*; (ii) only 20 out of the 52 ($\sim 40\%$) ISOCAM sources detected in the upper 1.5 bolometric magnitudes of the RGB ($M_{\text{bol}} \leq -2.5$) show evidence of circumstellar dust excess; by correcting for stars not detected because of the low spatial resolution of ISOCAM, dusty envelopes are inferred around about 15% of the brightest giants, this suggests that *the mass loss process is episodic*; (iii) *there is no evidence of any dependence of mass loss occurrence on the cluster metallicity*.

4. UV observations: probing the hot stellar population in GGCs

Although the CMD of an old stellar population (as a GGC) is dominated, in the *classical* $(V, B - V)$ -plane, by the cool stellar component, relatively populous hot stellar components do exist in GGCs and are strong emitters in the UV (hot post-Asymptotic Giant Branch stars, blue HB, BSS, various by-products of binary system evolution, and so on).

The advent of the Hubble Space Telescope (HST), with its unprecedented spatial resolution and imaging/spectroscopic capabilities in the UV, has given a new impulse to the study of hot stars in GGCs. We are involved in a long-term observational programme which uses HST to perform UV observations in a selected sample of GGCs. In this section I summarize the most recent results obtained for BSS (a few additional results on the search of peculiar objects can

be found in the poster contribution by Sabbi et al. and Ferraro et al. in this book).

4.1. Blue Straggler Stars in the UV

Blue Straggler stars (BSS), first discovered by Sandage (1953) in M3, are commonly defined as stars brighter and bluer (hotter) than the main sequence (MS) turnoff (TO), lying along an apparent extension of the MS, and thus mimicking a rejuvenated stellar population. The existence of such a population has been a puzzle for many years, and even now its formation mechanism is not completely understood, yet. At present, the leading explanations involve mass transfer between binary companions or the merger of a binary star system or the collision of stars (whether or not in a binary system). Direct measurements (Shara et al. 1997; Gilliland et al. 1998) and indirect evidence have in fact shown that BSS are more massive than the normal MS stars, pointing again toward a collision or merger of stars. Thus, the BSS represent the link between classical stellar evolution and dynamical processes (see Bailyn 1995). The realization that BSS are the ideal diagnostic tool for a quantitative evaluation of the dynamical interaction effects inside star clusters has led to a remarkable burst of searches and systematic studies, using UV and optical broad-band photometry.

Our group has actively participated to this extensive surveys and has published some of the first and most complete catalogs of BSS in GCs (Fusi Pecci et al 1992; Ferraro, Bellazzini & Fusi Pecci 1995; Ferraro et al 2002). These works have significantly contributed to form the nowadays commonly accepted idea that BSS are indeed a normal component of stellar populations in clusters, since they are present in all of the properly observed GGCs. However, according to Fusi Pecci et al. (1992) BSS in different environments could have different origin. In particular, BSS in loose GGCs might be produced from coalescence of primordial binaries, while in high density GGCs (depending on survival-destruction rates for primordial binaries) BSS might arise mostly from stellar interactions, particularly those which involve binaries. Thus, while the suggested mechanisms for BSS formation could be at work in clusters with different environments (Ferraro, Bellazzini, & Fusi Pecci, 1995; Ferraro et al. 1999) there is evidence that they could also act simultaneously within the same cluster (as in the case of M3, see Ferraro et al. 1993; Ferraro et al. 1997). Moreover, as shown by Ferraro et al. (2002), both the BSS formation channels (primordial binary coalescence and stellar interactions) seem to be equally efficient in producing BSS in different environments, since the two clusters that show the largest known BSS specific frequency, i.e. NGC 288 (Bellazzini et al. 2002) and M 80 (Ferraro et al. 1999), represent two extreme cases of central density concentration among the GGCs ($\text{Log}\rho_0 = 2.1$ and 5.8). Particularly interesting is the case of M80 which shows an exceptionally high BSS content: more than 300 BSS have been discovered in M80 (Ferraro et al 1999). This is *the largest and most concentrated BSS population ever found in a GGC*. Since M80 is the GGC which has the largest central density among those not yet core-collapsed, this discovery could be the first direct evidence that stellar collisions could indeed be effective in delaying the core collapse.

Figure 4 shows the (m_{255} , $m_{255} - m_{336}$) CMDs for six clusters observed in the UV with HST (Ferraro et al 2002). More than 50,000 stars are plotted

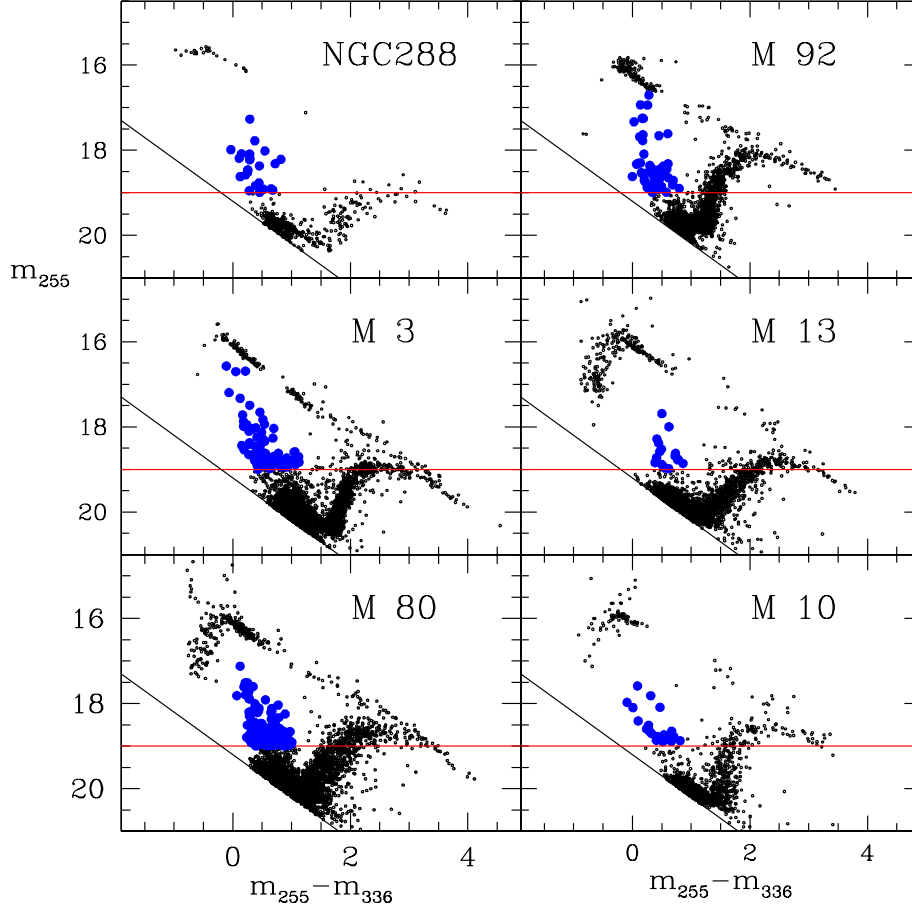


Figure 4. $(m_{255}, m_{255} - m_{336})$ CMDs for the 6 clusters observed with HST. Horizontal and vertical shifts have been applied to all CMDs in order to match the main sequences of M3. The horizontal solid line corresponds to $m_{255} = 19$. The bright BSS candidates are marked as large filled circles (from Ferraro et al 2002).

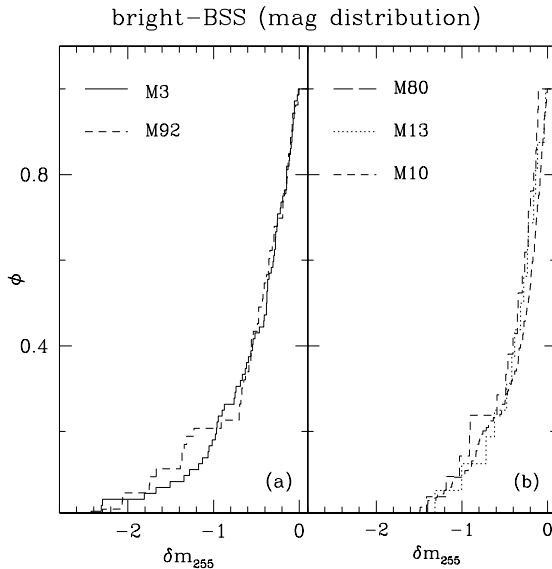


Figure 5. Cumulative magnitude distributions for the *bright* BSS for each of the six clusters. The δm_{255} parameter is the b-BSS magnitude with respect to the threshold ($m_{255} = 19$). In *Panel (a)* the BSS distributions for M3 and M92 (the two clusters for which the BSS distribution extends up to more than two magnitudes brighter than the threshold) are compared. In *Panel (b)* the BSS magnitude distributions for the other 3 clusters are plotted.

in the six panels of Figure 4. The CMD of each cluster has been shifted to match that of M3 using the brightest portion of the HB as the normalization region. The solid horizontal line (at $m_{255} = 19$) in the figure shows the threshold magnitude for the selection of bright (hereafter bBSS) sample. Such a dataset allows a direct comparison of the photometric properties of bBSS in different clusters. In particular, we have found evidence (Ferraro et al. 2002) for a possible connection between the presence of a blue tail in the HB and the BSS UV-magnitude distribution: GGCs without HB blue tails have BSS-Luminosity Function (LF) extending to brighter UV magnitudes with respect to GGCs with blue tails.

In Figure 5 the magnitude distributions (equivalent to a LF) of bBSS for the six clusters are compared. In doing this we use the parameter δm_{255} defined as the magnitude of each bBSS (after the alignment showed in Figure 4) with respect to the magnitude threshold (assumed at $m_{255} = 19$ - see Figure 4). Then $\delta m_{255} = m_{255}^{bBSS} - 19.0$. From the comparison shown in Figure 5 (*panel(a)*) the bBSS magnitude distributions for M3 and M92 appear to be quite similar and both are significantly different from those obtained in the other clusters. This is essentially because in both clusters the bBSS magnitude distribution seems to have a tail extending to brighter magnitudes (the bBSS magnitude tip reaches $\delta m_{255} \sim -2.5$). A KS test applied to these two distributions yields a probability of 93% that they are extracted from the same distribution. In *panel(b)* we see that the bBSS magnitude distribution of M13, M10 and M80 are essentially indistinguishable from each other and significantly different from M3 and M92.

A KS test applied to the three LFs confirms that they are extracted from the same parent distribution. Moreover, a KS test applied to the total LFs obtained by combining the data for the two groups: M3 and M92 (*group(a)*), and M13, M80 and M10 (*group(b)*) shows that the the bBSS-LFs of *group(a)* and *group(b)* are not compatible (at 3σ level).

It is interesting to note that the clusters grouped on the basis of bBSS-LFs have some similarities in their HB morphology. The three clusters of *group(b)* have an extended HB blue tail; the two clusters of *group(a)* have no HB extension. Could there be a connection between the bBSS photometric properties and the HB morphology? This possibility needs to be further investigated.

Acknowledgments. It is a pleasure to thank all the collaborators involved in this vast project. In particular, I want to thank Elena Pancino for a critical reading of this manuscript and Livia Origlia for her continuous support. The financial support of the *Agenzia Spaziale Italiana* (ASI) and of the *Ministero della Istruzione dell'Università e della Ricerca* (MIUR) is kindly acknowledged.

References

- Bailyn, C.D.: 1995, *ARA&A*, 33, 133
 Bellazzini, M., et al., 2002, *AJ*, 123, 1509
 Davidge, T.J., 2000, *ApJSS*, 126, 105
 Ferraro, F.R., et al, 1993, *AJ*, 106, 2324
 Ferraro, F.R., Fusi Pecci, F. & Bellazzini, M. 1995, *A&A*, 294, 80
 Ferraro, F.R., et al., 1997a, *A&A*, 320, 757
 Ferraro, F.R., et al., 1999a, *AJ*, 118, 1783 (F99)
 Ferraro, F.R., et al., 1999b, *ApJ*, 522, 983
 Ferraro, F.R., et al., 2000 *AJ*, 119, 1282 (F00)
 Ferraro, F.R., et al., 2002, *ApJ*, submitted
 Frogel J.A., Cohen J.G., Persson S.E., 1983, *ApJ* 275, 773
 Frogel J.A., et al 1995, *AJ*, 109, 1154
 Fusi Pecci, F., et al., 1992, *AJ*, 104, 1831
 Gilliland, R.L., 1998, *ApJ*, 507, 818
 Kuchinski L.E. & Frogel J.A., 1995, *AJ*, 110, 2844
 Lee, Y-W., et al., 1999, *Nature*, 402, 55
 Minniti D., et al., 1995, *AJ*, 110, 1686
 Origlia, L., et al., 2002, *ApJ*, 571, 458
 Ortolani, S., 2001, *A&A*, 376, 878
 Pancino et al 2000, *ApJ*, 534, L83
 Pancino et al 2002, *ApJ*, 568, L101
 Sandage, A., 1953, *AJ*, 58, 61
 Shara, R.A., et al, 1997, *ApJ*, 489, L59